



New type of RNA virus replication inhibitor based on decahydro-*closo*-decaborate anion containing amino acid ester pendant group

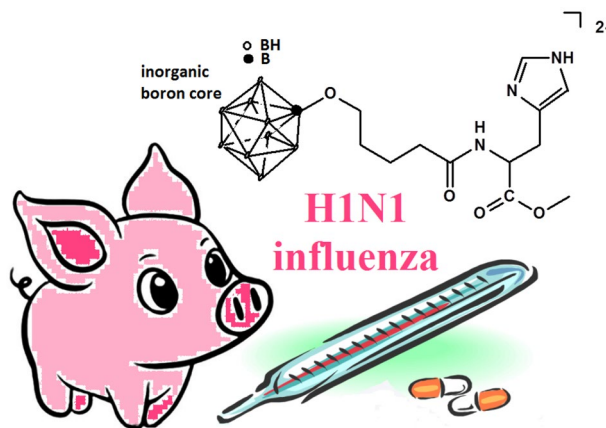
Varvara V. Avdeeva¹ · Timur M. Garaev² · Natalia V. Breslav² · Elena I. Burtseva² · Tatyana V. Grebennikova² · Andrei P. Zhdanov¹ · Konstantin Yu. Zhizhin¹ · Elena A. Malinina¹ · Nikolay T. Kuznetsov¹

Received: 12 October 2021 / Accepted: 3 March 2022 / Published online: 25 March 2022
© The Author(s), under exclusive licence to Society for Biological Inorganic Chemistry (SBIC) 2022

Abstract

In this work, a synthetic approach to prepare an example of new class of the derivatives of the *closo*-decaborate anion with amino acids detached from the boron cluster by pendant group has been proposed and implemented. Compound $\text{Na}_2[\text{B}_{10}\text{H}_9\text{-O}(\text{CH}_2)_4\text{C}(\text{O})\text{-His-OMe}]$ was isolated and characterized. This compound has an inorganic hydrophobic core which is the 10-vertex boron cage and the $\text{-O}(\text{CH}_2)_4\text{C}(\text{O})\text{-His-OMe}$ organic substituent. It has been shown to possess strong antiviral activity in vitro against modern strains of A/H1N1 virus at 10 and 5 $\mu\text{g}/\text{mL}$. The compound has been found to be non-cytotoxic up to 160 $\mu\text{g}/\text{mL}$. At the same time, the compound has been found to be inactive against SARS-CoV-2, indicating specific activity against RNA virus replication. Molecular docking of the target derivative of the *closo*-decaborate anion with a model of the transmembrane region of the M2 protein has been performed and the mechanism of its antiviral action is discussed.

Graphical Abstract



Keywords Decahydro-*closo*-decaborate anion · H1N1 virus · Molecular docking · Cytotoxicity · Boron clusters · Mechanism of action

✉ Varvara V. Avdeeva
avdeeva.varvara@mail.ru

Extended author information available on the last page of the article

Introduction

One of the most important tasks facing modern science in the twenty-first century is socially significant viral infections that worsen the quality of human life. These diseases

include viral hepatitis (primarily B and C), HIV infection, influenza A, etc. Vaccination as a method of combating socially significant infections is not always effective; therefore, the development of antiviral drugs remains an urgent task. The search and creation of chemical compounds capable of effectively interacting directly with a viral particle and thereby inhibit its replication process seems to be the most promising method for the treatment and prevention of socially significant viral infections.

Despite worldwide efforts to develop chemotherapy and vaccines, the 2009/2010 pandemic caused by the influenza A(H1N1)pdm2009 virus showed their extreme limitation and lack of effectiveness. New strains of the highly virulent influenza virus may appear unexpectedly and cause worldwide pandemics with high morbidity and mortality. Moreover, the danger of the appearance of A/H5N1 mutants, which can be transmitted from person to person, remains acute [1–4].

Rimantadine and its derivatives are active against a number of human viruses, including those that are part of the FDA-approved drugs against the influenza virus [5]. The mechanism of action of derivatives of adamantane, spiroadamantyl amine, and other framework compounds is associated with blocking the M2 ion channel of the virus [6–8]. Viroporin M2 is essential for the influenza virus to infect cells. This is an ion channel built into the viral envelope that selectively conducts protons from the cell into the virus. The virus enters the host cell enclosed in endosomes (membrane structures), which are a kind of vesicle. At a certain value of the acidity of the medium, the M2 protein is activated and begins to pump protons, lowering the pH inside the viral particle and thereby causing its decay. Thus, the genetic material of the virus is released into the cytoplasm of the host cell [9].

Recently, using the methods of real-time nuclear magnetic resonance (NMR), a detailed structure of the M2 protein has been determined which allows one to understand the molecular mechanism that ensures the functioning of Viroporin M2 in the transfer of hydrogen ions. As a result, it was possible to confirm the previously proposed model. The driving force of this proton pump is concentrated in the

transmembrane region of the protein and is an imidazole conjugation of histidine residues at position 37 (His37). The source of protons is hydroxonium ions H_3O^+ [10].

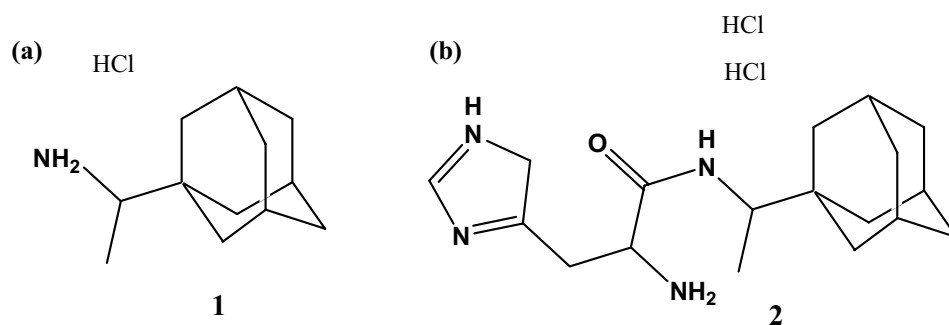
The residues of tryptophan at the 41st position in the transmembrane region close the channel pore from the inside. When three or all four imidazoles are protonated, electrostatic repulsion arises between the imidazoles. This in turn violates the helical packing of the chains of the tetrameric channel M2 and opens a portal of Trp41 indoles for the passage of protons inside the viral particle. Violation of this mechanism should allow the creation of an effective drug against influenza, even for strains that have become resistant to the effects of existing drugs [11].

Recent studies of adamantane and norbornene derivatives containing amino acid and peptide esters have shown that these compounds have antiviral activity against influenza strains A/H1N1pdm2009, A/H3N2 and A/H5N1 [12]. Amino acids and other physiologically active compounds were condensed with rimantadine (**1**) (Fig. 1a) by peptide synthesis methods. In previous studies, the biological compound L-histidyl-1-adamantyl ethylamine ($2\text{HCl} \cdot \text{H-His-Rim}$, **2**) [12] (Fig. 1b) was selected as a result of biological screening; it was found to be an inhibitor of the M2 channel function of influenza A virus resistant drugs of the adamantane series [13].

Here, we proposed to use the *clos*o-decaborate anion $[\text{B}_{10}\text{H}_{10}]^{2-}$ as an inorganic membranotropic carrier of the same functional groups instead of organic adamantane to create a promising antiviral drug.

Boron cluster anions $[\text{B}_n\text{H}_n]^{2-}$ ($n=6-12$) [14–17] attract attention of chemists because they provide wide opportunities to vary their structure and potential application. The chemical behavior of boron cluster anions and their derivatives (kinetic stability, thermal stability, a variety of substitution reactions [18–23]) results first from their three-dimensional aromaticity [24–27]. Modern application of boron clusters includes radionuclide diagnostics and therapy, ionic liquids, extraction of radionuclides, energetic materials, preparation of neutron-protective coatings, catalysis, application as pharmacophores, scaffolds in molecular construction, modulators of bioactive compounds [28–40]. In

Fig. 1 a Molecule of rimantadine (**1**) (Rim) and b $2\text{HCl} \cdot \text{H-His-Rim}$ (**2**)



addition, the boron clusters and carboranes can be used in biological imaging [41, 42] and highly efficient molecular magnets have been developed based on them [43–45].

A number of compounds containing boron clusters were shown to possess antiviral activity. In particular, a series of conjugates of *para*-carborane [46], *ortho*-carborane [47], and cobalt bis(1,2-dicarbollide) [48] with 5-ethynyl-uridine were prepared by Sonogashira coupling of the corresponding boron cage-containing terminal alkynes and 5-iodo-nucleoside and were studied to have activity against HCMV, EMCV, HPIV-3, HSV-1; the designed compounds demonstrated low to moderate cytotoxicity in several cell lines. The most potent compound is 5-[(1,12-dicarba-*closo*-dodecaboran-2-yl)ethyn-1-yl]-20-deoxyuridine with an IC₅₀ value of 5.5 mM and a selectivity index higher than 180; it exhibits antiviral activity against HCMV but is not active against HSV-1, HPIV-3 or EMCV [49]. In addition, carborane ester of oseltamivir carboxylic acid was described as novel neuraminidase inhibitor [50], which was found to be an order of magnitude less active than its precursor, the corresponding ethyl ester, which is the active principle of pharmaceutical preparations used in influenza prophylactics and therapy. Moreover, *closo*-dodecaborate conjugates based on *closo*-dodecaborate amines as a versatile synthons were prepared, including bis-(*closo*-dodecaborates), *closo*-dodecaborate conjugates with lipids, and with a non-natural nucleoside, 8-aza-7-deaza-2'-deoxyadenosine. No antiviral activity was detected for the tested compounds (HSV-1, HPIV-3 or EMCV, VSV, HMCV) [50].

Recently, we discussed the idea to create the peptide bond in derivatives of the *closo*-decaborate anion by using a multi-step synthesis based on the nucleophilic addition of amino acid derivatives to the [2-B₁₀H₉NCCH₃][−] anion to form N-borylated dipeptide R-GlyPheOEt [51]. The amino acid residue was introduced into the boron cage through the amidine fragment. However, these compounds have not been studied for antiviral or antimicrobial activity.

In the present work, the derivative of the *closo*-decaborate anion [B₁₀H₁₀]^{2−} with histidine methyl ester (H-His-OMe) detached from the boron cluster by the alkoxy spacer was synthesized and its antiviral activity against A/H1N1 and SARS-CoV-2 was studied.

Experimental

Materials

Solvents (HPLC grade) and solids (Bu₄N)CN (95%), L-histidine methyl ester dihydrochloride (97%), 1-ethyl-3-(3-dimethylaminopropyl)carbodiimide (97%), 1-hydroxybenzotriazole (97%), 4-dimethylaminopyridine (99%), sodium tetraphenylborate (99%) were purchased from Sigma-Aldrich

and used without additional purification. [Et₃NH]₂[B₁₀H₁₀] was prepared from decaborane-14 using the known synthetic procedure [52]. (Bu₄N)[B₁₀H₁₁] was prepared by protonation of the [B₁₀H₁₀]^{2−} anion in the CH₃CN/CF₃COOH system according to the method reported [53]. (Bu₄N)[2-B₁₀H₉O(C₄H₈)] was synthesized from (Bu₄N)[B₁₀H₁₁] and THF according to the known procedure [54]. The substitute was opened to give (Bu₄N)₂[2-B₁₀H₉OC₄H₈CN] when reacting with (Bu₄N)CN in dichloromethane [55]; (Bu₄N)₂[2-B₁₀H₉OC₄H₈COOH] was obtained [55] by hydrolysis in boiled methanol with KOH.

Racemic **rimantadine hydrochloride** purchased from Zhejiang Kangyu Pharmaceutical Co (China) and **hydroxy-chloroquine sulfate** purchased from Promochem (Finland) were used as reference drugs.

Synthesis

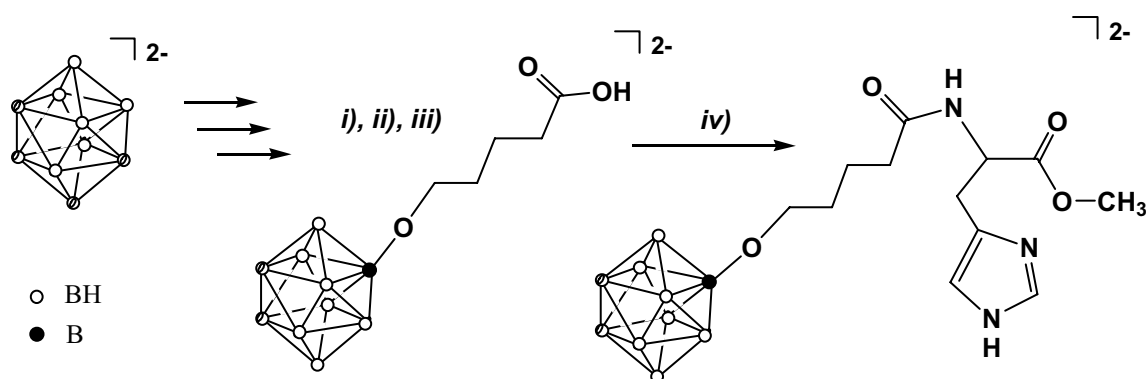
(Bu₄N)₂[2-B₁₀H₉OC₄H₈CONHCH(COOMe)CH₂(4-1H-Imidazole)], (Bu₄N)₂An

(Bu₄N)₂[2-B₁₀H₉OC₄H₈COOH] (2.00 g; 2.8 mmol) was dissolved in 30 ml of 1,2-dichloroethane. The obtained solution was cooled to 0 °C, then HOBT (1-hydroxybenzotriazole) (80 wt%, 0.71 g; 4.2 mmol), EDC HCl (1-ethyl-3-(3-dimethylaminopropyl)carbodiimide) (0.65 g; 4.2 mmol) and DMAP (4-dimethylaminopyridine) (1.22 g; 10.0 mmol) were added. The resulting reaction mixture was stirred for 30 min in a dry argon atmosphere. Then L-histidine methyl ester dihydrochloride (1.02 g; 4.2 mmol) was added to the mixture. The reaction mixture was warmed to room temperature and stirred 12 h. The formed precipitate of dimethylaminopyridine hydrochloride was filtered off; the mother liquor was concentrated on a rotary evaporator. The dry residue was treated with water and extracted with dichloromethane. The organic fractions were washed sequentially with 0.1 M HCl and water, then dried over sodium sulfate and concentrated on a rotary evaporator. The product was dried under oil pump vacuum. Yield, 2.25 g (92%).

MS (ESI) *m/z*: 384.3 ({A-H})[−] refers to the molecular weight of [C₁₂H₂₇B₁₀N₃O₄]^{2−}, calculated for {[A][−]} 384.5). **Anal. Calcd.** for C₄₄H₉₃B₁₀N₅O₄, (444.7): C, 60.98; H, 10.83; N, 8.09; B, 12.7. **Found**: C, 60.96; H, 10.86; N, 8.12; B, 12.6. **IR** (KBr, cm^{−1}, selected bands): ν(NH) 3239, ν(BH) 2481, ν(C=N amide) 1635, ν(C=N imidazole) 1562, ν(BO) 1383.

Na₂[2-B₁₀H₉OC₄H₈CONHCH(COOMe)CH₂(4-1H-Imidazole)], Na₂An

Sodium salt Na₂An was prepared by treating (Bu₄N)₂An with aqueous sodium tetraphenylborate (TPB), filtration of precipitated (Bu₄N)TPB, and evaporation of water from the



i) CF₃COOH, HCOOH, THF, ii) (Bu₄N)CN, CH₂Cl₂, iii) KOH, THF/H₂O, iv) DMAP, EDC·HCl, HOBT, HisOMe·2HCl

Scheme 1. Preparation of target derivative (Bu₄N)₂An

resulting filtrate resulting in the target compound as white powder. Yield, 85%. ¹¹B[¹H]-NMR (D₂O/CD₃OD) δ (ppm): – 2.1 (s, 1B, B(2)), – 3.9, – 4.6 (s, 2B, B(1) + B(10)), – 24.3 (s, 4B, B(3,5,6,9)), – 30.0 (s, 2B, B(7,8)), – 35.2 (s, 1B, B(4)).

Physicochemical methods

Infrared spectra of compounds were recorded on an Lumex InfraLum FT-02 FT-IR spectrometer (St.-Petersburg, Russia) in the range 4000–400 cm⁻¹ (Nujol, KBr pellets).

The elemental analysis of compounds was carried out on a Carlo Erba Instruments EA1108 automatic CHN analyzer; the samples were preliminary heated to constant weight. **Determination of boron** was performed by electrothermal atomic absorption on a Perkin-Elmer 2100 spectrophotometer with an HGA-700 furnace.

Mass spectra of the reaction solutions in CH₃CN were recorded on an API 3200 Qtrap spectrometer (Applied Biosystem, USA). Ionization conditions: turbo ion sputtering, ion sputtering, voltage ±4500 V, declustering ± 12 V, flow rate 2–20 μL/min. The average analytical concentration of samples was 0.5–1.0 mg/L.

¹H, ¹³C and ¹¹B[¹H] NMR spectra of solutions of the studied substances in CD₃CN and D₂O/CD₃OD were recorded on a Bruker MSL-300 pulsed Fourier spectrometer (Germany) at frequencies of 300.3, 75.49 and 96.32 MHz, respectively, with internal deuterium stabilization. Tetramethylsilane or boron trifluoride ether was used as the external standard, respectively. The NMR spectroscopy data for Na₂An are described in Supplementary Information (see Figs. S1–S3).

Calculation details

Methodology for conducting quantum chemical calculations

The full geometry optimization of the ligand An²⁻ has been carried out at the ωB97X-D3/6–31 + G(d,p) level of theory with the help of the ORCA 4.2.1 program package [56]. The quantum–mechanical model of the ligand An²⁻ was generated in HyperChem 8.0.8 software product by Hypercube [57].

Molecular docking

The structure of the transmembrane domain M2 S31N from RCSB Protein Data Bank (structure code 2KIH) was taken as a target for docking to be performed. The transmembrane domain M2 S31N contained the S31N mutation, which is a marker of strain resistance to rimantadine and amantadine. Molecular docking was carried out using the online service PatchDock (Molecular Docking Algorithm Based on Shape Complementarity Principles) [58].

Procedures of **biological experiments** and **determination of antiviral activity** are described in Supporting Information.

Results and discussion

The target compound (Bu₄N)₂An was synthesized from (Bu₄N)[B₁₀H₁₁] according to Scheme 1. The process control at each stage was carried out using ¹¹B NMR spectroscopy and TLC.

The structure of the substituted *closo*-decaborate (Bu_4N)₂**An** with a peptide functional group was determined using multinuclear NMR spectroscopy (see Supplementary Information) and IR spectroscopy. The introduction of a peptide group into the cluster cage has no effect on the shape of the ¹¹B NMR spectrum; it is a spectrum of “classical” mono-substituted derivative of the *closo*-decaborate anion. In the IR spectrum of compound (Bu_4N)₂**An**, a broad band of the BH groups $\nu(\text{BH})$ is observed at 2481 cm^{-1} , whereas a band of stretching vibrations of the B–O group $\nu(\text{BO})$ appears at 1383 cm^{-1} . The $\nu(\text{C}=\text{N}$ amide) and $\nu(\text{C}=\text{N}$ imidazole) stretching vibrations are observed at 1635 and 1562 cm^{-1} , respectively. A band with maximum at 3239 cm^{-1} corresponds to $\nu(\text{NH})$ stretching vibrations.

Sodium salt Na_2An was prepared by treating (Bu_4N)₂**An** with aqueous sodium tetraphenylborate (TPB), filtration of (Bu_4N)TPB precipitated, and evaporation of water from the resulting filtrate resulting in the target compound as white powder. The ¹¹B NMR and IR spectra of Na_2An are similar to those of (Bu_4N)₂**An**; in ¹H and ¹³C NMR spectra, all the peaks corresponding to the boron cluster derivative **An**²⁻ are present, while no signals corresponding to the (Bu_4N)⁺ cations are observed (Figs. S1–S3).

The antiviral activity of Na_2An against virus IIV-A/Moscow/01/2009(H1N1)pdm09 was studied by ELISA according to standard methods [58, 59].

As it was indicated, L-histidyl-1-adamantylethylamine ($\text{HCl}\cdot\text{H-His-Rim}$) (Fig. 1b) showed the best antiviral activity among a number of adamantane and norbornene derivatives containing amino acid and peptide esters [12, 13]. Therefore, we believe that the antiviral activity of novel drug Na_2An should be studied in comparison with $\text{HCl}\cdot\text{H-His-Rim}$ (**1**).

Table 1 presents the antiviral activity of compound Na_2An in comparison with **1** and the reference drug rimantadine hydrochloride (**2**).

Na_2An was shown the highest antiviral activity, at both 10.0 and 5.0 $\mu\text{g}/\text{mL}$. The compound has a cytotoxic dose > 160 $\mu\text{g}/\text{ml}$ as established by the MTT method, which undoubtedly opens the possibility of obtaining a drug with a high selectivity index. The lack of antiviral properties of

rimantadine (**2**) proves that a resistant strain of influenza A virus was used in the experiment.

We believe that the mechanism of action of the derivative **An**²⁻ on influenza A virus should be similar to the effect of rimantadine/amantadine on the M2 channel of influenza A virus [9–11, 60]. In those studies, viroporins were assumed the target of the antiviral activity. Viroporins are widely involved in the interaction of viruses with the cell at various stages. The function of several viroporins in vitro is inhibited by the non-specific antiviral drug amantadine (1-aminoadamantane) [61], which indicates the direction of the development of new broad-spectrum antiviral drugs.

The molecular model of the inhibitor of the viroporin transport function assumed the presence of a hydrophobic core of carbocyclic alkanes (adamantane, norbornene) [12, 13] or other condensed and mixed aromatic systems. The carbocyclic component of the molecule acts as a membranotropic carrier for the functional group capable of forming a non-covalent interaction with the protein surface of the viropore channel pore. The molecular mechanism showing the functioning of Viroporin M2 in the transfer of hydrogen ions is present in Fig. S4. The functional group of the molecule can be represented by amino acids, peptides and a number of other physiologically active compounds that can act as a source of such groups. In this case we used the *closo*-decaborate anion as a carrier and His-OMe as a functional group.

In silico studies have been conducted to propose the mechanism of the action of anion **An**²⁻. According to our concept of the molecular design of a molecule that should inhibit the M2 channel function of the influenza A virus, the boron cluster as a membranotropic carrier should “drag” the functional group (in our case, the His residue) into the pore of the M2 channel. This model was built using the PM3 semi-empirical quantum mechanical calculation method. The calculation was carried out only for valence electrons; integrals of certain interactions were neglected; standard non-optimized basis functions of electron orbitals were used, and the main parameters used for PM3 were obtained by comparing a large number and type of experiments with the results of calculations. The resulting model is shown in

Table 1 Percentage of inhibition of reproduction of the pandemic strain of the influenza virus IIV-A/Moscow/01/2009(H1N1)pdm09 by compounds **1**, **2**, and Na_2An in the MDCK cell culture: **1** is $\text{HCl}\cdot\text{H-His-Rim}$, **2** is $\text{Rim}\cdot\text{HCl}$, and Na_2An is $\text{Na}_2[\text{B}_{10}\text{H}_9\text{-O}(\text{CH}_2)_4\text{HisOMe}]$

Virus dilution	Percentage of inhibition of viral reproduction, %					
	Drugs, $\mu\text{g}/\text{mL}$					
	Na_2An		1		2	
	5.0	10.0	5.0	10.0	5.0	10.0
10^{-2}	91.0	88.0	47.0	62.0	0	0
10^{-3}	91.0	96.0	40.0	58.0	0	0

Fig. 2a. The result of docking is the binding energy of the ligand with the active site in the conformation providing the best interaction of the ligand with the protein binding site. The location of An^{2-} in the pore of the M2 channel is shown in Fig. 2b.

In general, all molecular docking solutions can be divided into two groups in which the boron cluster is directed deep into the channel and vice versa towards the outside of the M2 channel of the influenza A virus (Table S1). The orientation of the ligand molecule with the boron cluster directed into the M2 channel seems to be the most promising solution. In this case, the boron cluster An^{2-} acts as a membranotropic carrier for the histidine residue.

Nevertheless, it should be noted that for the inward orientation of the drug, i.e. with the boron cage directed towards the channel input (Solution 1 from Table S1, Fig. S5), the energetic and spatial characteristics are slightly higher than for the arrangement of the compound with the boron cluster for the downward orientation (Solution 2 from Table S1, Fig. S6). Probably, a small size of the anion An^{2-} , as well as the flexibility of the hydrocarbon chain of the side groups, allow the ligand to turn round in the pore of the M2 channel. Therefore, the introduction of the ligand into the pore still occurs through the carrier (the *closo*-decaborate anion) followed by the turning of the molecule under the action of the internal forces of the proton pump. These assumptions have to be tested in terms of the calculation of Molecular Dynamics, which allow visualizing the process of interaction between the drug and the target protein [62].

On the other hand, the new human coronavirus SARS-CoV-2, as well as the MERS and SARS viruses, contains an ion-selective channels (viroporins of protein E and protein 3C). Pentameric structure of the E protein also has an alpha helix in the transmembrane domain (TM) [63]. The

viroporin E of the coronavirus, in contrast to the M2 protein, is post-translational, i.e. is not contained in the envelope of the virus, but acts at the stage of assembly of virions [64]. Protein E is localized in the intermediate compartment between the endoplasmic reticulum and the Golgi complex (ER-Golgi), where coronavirus virions gather and mature to exit the infected cell. Moreover, the E protein is involved in blocking cell apoptosis [65, 66]. Thus, blocking the action of this viroporin could possibly significantly impair the reproduction of SARS-CoV-2, as compared to the antimalarial drug hydroxychloroquine [67]. As a result of the study of the antiviral activity of Na_2An in in vitro experiments against SARS-CoV-2, no statistically significant antiviral effect was found in the protocols of adding the target drug 24 h before, simultaneously, and 24 h after infection, because a decrease in the infectious titer of the virus by at least 2.0 lg was not achieved (Table 2).

Conclusions

In this work, we proposed a method for the synthesis of the $[\text{B}_{10}\text{H}_9\text{-O}(\text{CH}_2)_4\text{C}(\text{O})\text{-His-OMe}]^{2-}$ anion, which is a substituted derivative of the *closo*-decaborate anion with the His-OMe functional group separated from the boron cluster by the $\text{O}(\text{CH}_2)_4$ spacer. Biological tests performed in vitro for the sodium salt to find antiviral properties against influenza A/H1N1 and SARS-CoV-2 viruses demonstrated that the key compound has antiviral activity against influenza A/H1N1 at concentrations of 10 and 5 $\mu\text{g}/\text{ml}$. The 50% cytotoxic concentration (CC_{50}) of the compound against MDCK cells was 160 $\mu\text{g}/\text{mL}$, and the selectivity index (SI) was over 32. Based on the data obtained by molecular docking of the boron cluster anion with the model of the transmembrane region of the M2 protein, a mechanism for the antiviral action of the boron cluster was proposed.

Thus, one could expect antiviral properties for derivatives of the decahydro-*closo*-decaborate anion with pendant amino acids, peptides, and some other physiologically important compounds, because the boron cage acts as a membranotropic carrier. This agrees with the proposed inhibitor model, and the derivatives discussed can be considered as a new class of objects with promising antiviral activity. Moreover, it should be emphasized that the data obtained for the influenza A virus is fundamentally different from the data obtained for the inhibition of SARS-CoV-2 replication, which indicates the selectivity of the effect of Na_2An on the influenza A virus.

Supporting Information contains Molecular Docking Algorithm solutions (Table S1), details of biological experiments and determination of antiviral activity, ^{11}B , ^1H , and ^{13}C NMR spectra of Na_2An (Figs. S1–S3), proton channel of influenza virus A (Fig. S4) and that with inserted drug

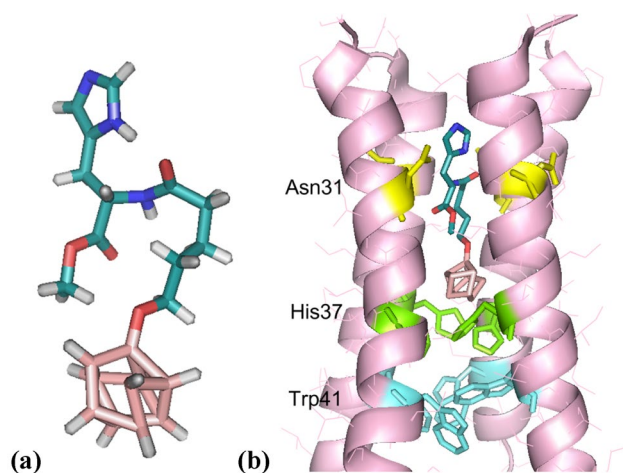


Fig. 2 **a** Model of anion An^{2-} with optimized geometry involved in docking and **b** quantum-mechanical model of the complex of the M2 protein and drug An^{2-}

Table 2 Effect of compound Na₂An on SARS-CoV-2 reproduction in Vero E6 cell culture

Drug concentration	TCID ₅₀ , lg	Virus control, lg	Δlg _{max} the maximum decrease in the value of the infectious viral dose in the experiment compared to the control, expressed in decimal logarithms
Administration of drug 24 h before infection			
50.0 µg/ml	6.67	7.33	0.66
25.0 µg/ml	7.33	7.33	0
Administration of drug simultaneously with infection			
50.0 µg/ml	6.67	7.33	0.66
25.0 µg/ml	7.33	7.33	0
Administration of drug 24 h after infection			
50.0 µg/ml	7.33	7.33	0
25.0 µg/ml	7.33	7.33	0
Reference drug – hydroxychloroquine			
12.9 µg/ml	0	5.67	5.67

An²⁻ containing the boron cluster in the inward orientation (Fig. S5) and downward orientation (Fig. S6) with respect to the channel input.

Supplementary Information The online version contains supplementary material available at <https://doi.org/10.1007/s00775-022-01937-4>.

Acknowledgements This work was supported by the Ministry of Science and Higher Education of the Russian Federation as part of the State Assignment of the Kurnakov Institute of General and Inorganic Chemistry of the Russian Academy of Sciences. The antiviral activity was studied as part of the State Assignment of the Gamaleya Federal Research Center for Epidemiology and Microbiology of the Ministry of Health of the Russian Federation (Russia). The authors are grateful to the scientific staff of the Laboratory of Influenza Etiology and Epidemiology of the Gamaleya Federal Research Center for Epidemiology and Microbiology of the Ministry of Health of the Russian Federation.

Author's contribution VVA: investigation, data curation, writing—review & editing; TMG: investigation, data curation, writing—original draft; NVB: investigation, data curation, EIB: formal analysis, visualization; TVG: supervision, APZ: investigation, data curation, writing—review & editing; KYZ: conceptualization; EAM: methodology; NTK: supervision.

Funding The synthetic part of the work was supported in part by the Russian Foundation for Basic Research, grants nos. 20-03-00763 and 19-29-08047 (Russia).

Declarations

Conflict of interest The authors declare that they have no conflicts of interest.

References

- Lanying Du, Li Ye, Zhao G, Wang L, Peng Zou LuLu, Zhou Y, Jiang S (2013) J Infect Dis 208:1315–1359. <https://doi.org/10.1093/infdis/jit323>
- Baldo V, Bertocello C, Cocchio S, Fonzo M, Pillon P, Buja A, Baldovin T (2016) J Prev Med Hyg 57:E19–E22
- Eyer L, Hruska K (2013) Vet Med 58:113–185. <https://doi.org/10.17221/6746-VETMED>
- Gonzalez MR, Bischofberger M, Pernot L, van der Goot FG, Frêche B (2008) Cell Mol Life Sci 65:493–507. <https://doi.org/10.1007/s00018-007-7434-y>
- Tompa DR, Immanuel A, Srikanth S, Kadhivel S (2021) Int J Biol Macromol 172:524–541. <https://doi.org/10.1016/j.ijbiomac.2021.01.076>
- Williams JK, Tietze D, Wang J, Yibing Wu, DeGrado WF, Hong M (2013) J Am Chem Soc 135:9885–9897. <https://doi.org/10.1021/ja4041412>
- Mandour YM, Breitinger U, Ma C, Wang J, Boeckler FM, Breitinger HG, Zlotos DP (2018) Drug Des Devel Ther 12:1019–1031. <https://doi.org/10.2147/DDDT.S157104>
- Chayrov R, Parisi NA, Chatziathanasiadou MV, Vrontaki E, Moschovou K, Melagraki G, Sbirikova-Dimitrova H, Shivachev B, Schmidtke M, Mitrev Y, Sticha M, Mavromoustakos T, Tzakos AG, Stankova I (2020) Molecules 25:3989. <https://doi.org/10.3390/molecules25173989>
- Yi M, Cross TA, Zhou HXJ (2008) Phys Chem B 112:7977–7979
- Miao Y, Fu R, Zhou HX et al (2015) Structure 23:2300–2308. <https://doi.org/10.1016/j.str.2015.09.011>
- Hu F, Luo W, Hong M (2010) Science 330:505–508. <https://doi.org/10.1126/science.1191714>
- Shibnev VA, Garaev TM, Finogenova MP, Shevchenko ES, Burtseva EI (2012) Bull Exp Biol Med 153:233–235. <https://doi.org/10.1007/s10517-012-1684-x>
- Shibnev VA, Deryabin PG, Garaev TM, Finogenova MP, Botikov AG, Mishin DV (2017) Russ J Bioorg Chem 43:517–525. <https://doi.org/10.1134/S1068162017050132>
- Muetterties EL, Knoth WH (1968) Polyhedral Boranes. Dekker, New York
- Greenwood NN, Earnshaw A (1997) Chemistry of the elements, 2nd ed., Butterworth-Heinemann
- Hosmane NS (ed) (2012) Boron science: new technologies and applications, 1st ed., CRC Press
- Boron-Based Compounds: Potential and Emerging Applications in Medicine, Eds. Hey-Hawkins E., Viñas Teixidor C. John Wiley & Sons Ltd., 2018. <https://doi.org/10.1002/9781119275602>
- Sivaev IB, Bregadze VI, Sjöberg S (2002) Collect Czech Chem Commun 67:679–727. <https://doi.org/10.1135/cccc20020679>

19. Sivaev IB, Prikaznov AV, Naoufal D (2010) Czech. Chem Commun 75:1149–1199. <https://doi.org/10.1135/cccc2010054>
20. Zhizhim KYu, Zhdanov AP, Kuznetsov NT (2010) Russ J Inorg Chem 55:2089–2127. <https://doi.org/10.1134/S0036023610140019>
21. Nelyubin AV, Selivanov NA, Bykov AY et al (2020) Russ J Inorg Chem 65:795–799. <https://doi.org/10.1134/S0036023620060133>
22. Nelyubin AV, Klyukin IN, Zhdanov AP et al (2021) Russ J Inorg Chem 66:139–145. <https://doi.org/10.1134/S0036023621020133>
23. Avdeeva VV, Malinina EA, Kuznetsov NT (2020) Russ J Inorg Chem 65:335–358. <https://doi.org/10.1134/S003602362003002X>
24. R. Bruce King, Chem. Rev. 101 (2001) 1119–1152. <https://doi.org/10.1021/cr000442t>
25. Chen Z, King RB (2005) Spherical aromaticity: recent work on fullerenes, polyhedral boranes, and related structures. Chem Rev 105:3613–3642. <https://doi.org/10.1021/cr0300892>
26. Ren L, Han Y, Hou X, Wu J (2021) All are aromatic: a 3D globally aromatic cage containing five types of 2D aromatic macrocycles. Chem 7:3442. <https://doi.org/10.1016/j.chempr.2021.11.003>
27. Poater J, Viñas C, Bennour I, Escayola S, Solà M, Teixidor F (2020) Too Persistent to Give Up: Aromaticity in Boron Clusters Survives Radical Structural Changes. J Am Chem Soc 142:9396–9407. <https://doi.org/10.1021/jacs.0c02228>
28. Sivaev IB (2017) Nitrogen heterocyclic salts of polyhedral borane anions: from ionic liquids to energetic materials. Chem Heterocycl Comp 53:638. <https://doi.org/10.1007/s10593-017-2106-9>
29. Teixidor F, Viñas C, Demonceau A, Núñez R (2003) Boron clusters: do they receive the deserved interest? Pure Appl Chem 75:1305. <https://doi.org/10.1351/pac200375091305>
30. Avdeeva VV, Garaev TM, Malinina EA, Zhizhin KYu, Kuznetsov NT (2022) Physiologically active compounds based on membranotropic cage carriers-derivatives of adamantane and polyhedral boron clusters (review). Russ J Inorg Chem 67:28–47. <https://doi.org/10.1134/S0036023622010028>
31. Ali F, Hosmane SN, Zhu Y (2020) Boron chemistry for medical applications. Molecules 25:828. <https://doi.org/10.3390/molecules25040828>
32. Sivaev IB, Bregadze VI (2009) Polyhedral boranes for medical applications: current status and perspectives. Eur J Inorg Chem. <https://doi.org/10.1002/ejic.200900003>
33. Abakumov GA, Piskunov AV, Cherkasov VK et al (2018) Organoelement chemistry: promising growth areas and challenges. Russ Chem Rev 87:393. <https://doi.org/10.1070/RCR4795>
34. Plešek J (1992) Potential applications of the boron cluster compounds. Chem Rev 92:269–278. <https://doi.org/10.1021/cr00010a005>
35. Duttwyler S (2018) Recent advances in B-H functionalization of icosahedral carboranes and boranes by transition metal catalysis. Pure Appl Chem 90:733. <https://doi.org/10.1515/pac-2017-1202>
36. Kuan Hu, Yang Z, Zhang L, Lin Xie Lu, Wang HX, Josephson L, Liang SH, Zhang M-R (2020) Boron agents for neutron capture therapy. Coord Chem Rev 405:213139. <https://doi.org/10.1016/j.ccr.2019.213139>
37. B. Sivaev, V. I. Bregadze, in Organometallic Chemistry Research Perspectives (Ed.: R. P. Irwin), Nova Publ., 2007, pp. 1–59
38. Sivaev IB, Bregadze VI, Kuznetsov NT (2002) Derivatives of the *closo*-dodecaborate anion and their application in medicine. Russ Chem Bull Int Ed 51:1362–1374
39. Leśnikowski ZJ (2016) Challenges and opportunities for the application of boron clusters in drug design. J Med Chem 59:7738–7758
40. Axtell JC, Saleh LM, Qian EA, Wixtrom AI, Spokoyniy AM (2018) Synthesis and applications of perfunctionalized boron clusters. Inorg Chem 57(5):2333–2350. <https://doi.org/10.1021/acs.inorgchem.7b02912>
41. Goswami LN, Ma L, Chakravarty S, Cai Q, Jalilati SS, Hawthorne MF (2013) Discrete nanomolecular polyhedral borane scaffold supporting multiple gadolinium(III) complexes as a high performance MRI contrast agent. Inorg Chem 52:1694–1700. <https://doi.org/10.1021/ic3017613>
42. Oña OB, Alcoba DR, Massaccesi GE, Torre A, Lain L, Melo JJ, Oliva-Enrich JM, Peralta JE (2020) Magnetic properties of *closo*-carborane-based Co(II) single-ion complexes with O, S, Se, and Te bridging atoms. Polyhedron 176:114257. <https://doi.org/10.1016/j.poly.2019.114257>
43. Oliva JM, Alcoba DR, Oña OB et al (2015) Toward (car)borane-based molecular magnets. Theor Chem Acc 134:9. <https://doi.org/10.1007/s00214-014-1611-5>
44. Belov AS, Voloshin YZ, Pavlov AA, Nelyubina YV, Belova SA, Zubavichus YV, Avdeeva VV, Efimov NN, Malinina EA, Zhizhin KYu, Kuznetsov NT (2020) Solvent-induced encapsulation of cobalt(II) ion by a boron-capped tris-pyrazoloximate. Inorg Chem 59(9):5845–5853. <https://doi.org/10.1021/acs.inorgchem.9b03335>
45. Białek-Pietrasa M, Olejniczak AB, Paradowska E, Studzińska M, Suski P, Jabłńska A, Leśnikowski ZJ (2015) J Organomet Chem 798:99–105
46. Białek-Pietrasa M, Olejniczak AB, Paradowska E, Studzińska M, Jabłńska A, Leśnikowski ZJ (2018) J Organomet Chem 865:166–172
47. Kosenko I, Ananyev I, Druzina A, Godovikov I, Laskova J, Bregadze V, Studzińska M, Paradowska E, Leśnikowski ZJ, Semioshkin A (2017) J Organomet Chem 849–850:142–149
48. Adamska A, Olejniczak AB, Zwoliński K, Szczepk WJ (2012) Ewelina Król3, Bogusław Szewczyk, Grzegorz Grynkiewicz, Zbigniew J Leśnikowski. Acta Poloniae Pharmaceuti Drug Res 69(6):1218–1223
49. Laskova J, Kozlova A, Białek-Pietras M, Studzińska M, Paradowska E, Bregadze V, Leśnikowski ZJ, Semioshkin A (2016) Reactions of *closo*-dodecaborate amines. J Organomet Chem 807:29–35
50. Nelyubin AV, Klyukin IN, Zhdanov AP et al (2019) Synthesis of substituted derivatives of *closo*-decaborate anion with a peptide bond: the way towards designing biologically active boron-containing compounds. Russ J Inorg Chem 64:1499–1506. <https://doi.org/10.1134/S003602361912012X>
51. Miller HC, Miller NE, Muettterties EL (1963) J Am Chem Soc 85:3885–3886
52. Mustyatsa VN, Votina NA, Goeva LV, Zhizhin KYu, Malinina EA, Kuznetsov NT (2001) Russ J Coord Chem 27:622
53. Zhizhin KYu, Mustyatsa VN, Malinina EA, Votina NA, Matveev EYu, Goeva LV, Polyakova IN, Kuznetsov NT (2004) Russ J Inorg Chem 49:180–189
54. Prikaznov AV, Shmal'ko AV, Sivaev IB, Petrovskii PV, Bragin VI, Kisin AV, Bregadze VV (2011). Polyhedron. <https://doi.org/10.1016/j.poly.2011.02.055>
55. Schneidman-Duhovny D, Inbar Y, Nussinov R, Wolfson HJ (2005) Nucl Acids Res 33:363–367. <https://doi.org/10.1093/nar/gki481>
56. Neese F (2012) The ORCA program system. WIREs Comput Mol Sci 2:73–78. <https://doi.org/10.1002/wcms.81>
57. Schneidman-Duhovny D, Yuval I, Nussinov R, Wolfson HJ (2005) Nucleic Acids Res 33:W363–W367. <https://doi.org/10.1093/nar/gki481>
58. Duff KC, Gilchrist PJ, Saxena AM, Bradshaw JP (1994) Virology 202:287–293. <https://doi.org/10.1006/viro.1994.1345>
59. Hay AJ, Wolstenholme AJ, Skehel JJ, Smith MH (1985) EMBO J 4:3021–3024. <https://doi.org/10.1002/j.1460-2075.1985.tb04038.x>
60. Wang C, Takeuchi K, Pinto LH, Lamb RA (1993) J Virol 67:5585–5594. <https://doi.org/10.1128/JVI.67.9.5585-5594.1993>
61. Cady SD, Mishanina TV, Hong M (2009) J Mol Biol 385:1127–1141. <https://doi.org/10.1016/j.jmb.2008.11.022>

62. Tzitzoglaki C, McGuire K, Lagarias P, Konstantinidi A, Hoffmann A, Fokina NA et al (2020) Chemical probes for blocking of influenza A M2 Wild-type and S31N channels. *ACS Chem Biol*. <https://doi.org/10.1021/acscchembio.0c00553>
63. Conzelmann C, Gilg A, Groß R, Schütz D, Preisling N, Ständker L, Jahrsdörfer B, Schrezenmeier H, Sparrer KMJ, Stamminger T, Stenger S, Münch J, Müller JA (2020) *Antiviral Res* 181:104882. <https://doi.org/10.1016/j.antiviral.2020.104882>
64. Tang T, Bidon M, Jaimes JA, Whittaker GR, Daniel S (2020) Coronavirus membrane fusion mechanism offers a potential target for antiviral development. *Antiviral Res* 178:104792. <https://doi.org/10.1016/j.antiviral.2020.104792>
65. Baguena CV, Nieto-Torres JL, Alcaraz A, DeDiego ML, Enjuanes L, Aguilera VM (2012) On channel activity of synthetic peptides derived from severe and acute respiratory syndrome coronavirus (SARS-CoV) E protein. *Biophys J* 102(3):656a–657a. <https://doi.org/10.1016/j.bpj.2011.11.3576>
66. Surya W, Li Y, Verdià-Bàguena C, Aguilera VM, Torres J (2015) MERS coronavirus envelope protein has a single transmembrane domain that forms pentameric ion channels. *Virus Res* 201(2):61–66. <https://doi.org/10.1016/j.virusres.2015.02.023>
67. Persoons L, Vanderlinden E, Vangeel L, Wang X, Do NDT, Foo SC, Leyssen P, Neyts J, Jochmans D, Schols D, De Jonghe S (2021) Broad spectrum anti-coronavirus activity of a series of anti-malaria quinoline analogues. *Antiviral Res* 193:105127. <https://doi.org/10.1016/j.antiviral.2021.105127>

Publisher's Note Springer Nature remains neutral with regard to jurisdictional claims in published maps and institutional affiliations.

Authors and Affiliations

Varvara V. Avdeeva¹  · Timur M. Garaev² · Natalia V. Breslav² · Elena I. Burtseva² · Tatyana V. Grebennikova² · Andrei P. Zhdanov¹ · Konstantin Yu. Zhizhin¹ · Elena A. Malinina¹ · Nikolay T. Kuznetsov¹

¹ Kurnakov Institute of General and Inorganic Chemistry, Russian Academy of Sciences, Leninskii pr. 31, Moscow 119991, Russia

² Gamaleya Federal Research Center for Epidemiology and Microbiology, Ministry of Health of Russian Federation, Moscow 123098, Russia